The Geode Process I: Hollow Silica Microcapsules as a High Surface Area Substrate for Semiconductor Nanowire Growth

Maritza Mujica, Gozde Tutuncuoglu, Amar T. Mohabir, Victor Breedveld, Sven H. Behrens and Michael A. Filler**

School of Chemical & Biomolecular Engineering, Georgia Institute of Technology, Atlanta 30332, Georgia, United States

KEYWORDS

semiconductor, nanowire, vapor-liquid-solid, emulsion templating, manufacturing

ABSTRACT

We introduce and demonstrate critical steps toward the Geode process for the bottom-up synthesis of semiconductor nanowires. Central to the process is the design and fabrication of an unconventional, high surface area substrate: the interior surface of hollow silica microcapsules, assembled from silica particles via emulsion templating, and featuring porous walls to enable efficient gas transport. The interior surface of these hollow silica microcapsules is decorated with gold nanoparticles that seed nanowire growth via the vapor-liquid-solid (VLS) mechanism. We demonstrate the production of the necessary microcapsules and show how microcapsule structure and stability upon drying is influenced by the type of silica particles and use of a particle cross-linking agent. Finally, we demonstrate the synthesis of Si nanowires in the microcapsule interior.

TEXT

Introduction

The bottom-up growth of semiconductor nanowires through the vapor-liquid-solid (VLS) mechanism offers exquisite control over nanowire structure and composition,[1-2] and thus functionality.[2-6] Demonstrations of prototype transistors,[7-10] photodetectors,[11-13] solar cells,[14-17] and biosensors[18-21], for example, highlight the promise of these materials for electronic, photonic, energy conversion, and medical applications. However, it remains difficult to produce nanowires in large quantities, especially those with the nanoscale compositional complexity required for the above applications. Most nanowires are grown on flat substrates.[22-24] Even with the adoption of roll-to-roll[25] and related high-throughput techniques,[26-27] scale-up of production rates in such processes is limited to L^2, where L is the characteristic size of the growth reactor. Significant productivity gains would come from decoupling the area of the nanowire growth substrate from the size of the reactor.

Here, we introduce the Geode process for the synthesis of semiconductor nanowires via the VLS mechanism. The basic concept is illustrated in Figure 1. We are inspired by natural geodes – hollow rocks whose inner surface serves as a site for the nucleation and growth of crystalline minerals as ions and water diffuse in/out of the cavity.[28-29] Producing hollow silica microcapsules with gold nanoparticles decorating their interior surfaces is accomplished with a scalable emulsion templating process.[30] Microcapsules are then placed inside a chemical vapor deposition furnace where diffusion of a reactive precursor gas through the porous microcapsule wall and its decomposition at the gold nanoparticles drive nanowire nucleation and growth.

The high surface area afforded by microcapsules is a key benefit of the Geode process. While the nanowire density possible per unit microcapsule surface area will likely be similar to that on flat substrates, the total surface area available inside a reactor filled with microcapsules can be substantially larger. The total surface area available in a small-scale, 1 ft^3 reactor filled with a powder of microcapsules (of similar dimensions to those reported here) is greater than 10,000 ft^2. This increase in total surface area and thus reactor productivity per volume is analogous to that routinely achieved by the chemical industry with heterogeneous catalytic nanoparticles dispersed inside inert, solid supports.[31-32]

Microcapsule powders offer benefits in addition to increased surface area. The anchoring of nanowires to the inner microcapsule surface limits nanowire agglomeration and nanowire-nanowire collisions that could perturb the seed particle. Microcapsules can also act as carriers for nanowires after synthesis, especially in cases where they need to undergo further processing steps. Moreover, powders consisting of particles with dimensions similar to our microcapsules can flow under a pressure gradient[33] or on a vibrating bed,[34] thus simplifying transport within a process or from step to step.

The Geode process aims to combine the efficiency of gas phase transport with the high productivity afforded by a very large substrate surface area. Solution-liquid-solid (SLS)[35-40] growth and Aerotaxy[41-43], two competing methods for scaling nanowire production, are likely limited in one of these regards. SLS is similar to VLS, except the growth precursors and the resulting nanowires occupy the bulk of a liquid phase. However, this means that SLS must contend with precursor transport rates orders of magnitude slower than those in the gas phase. The inefficiency of precursor addition and removal impedes the fabrication of nanowires with controlled nanoscale heterogeneity, which benefits from rapid precursor switching. Solvent and

surfactant use/removal can also be costly at industrially-relevant manufacturing scales.[44] The second approach, Aerotaxy, is a derivative of the so-called "floating catalyst" method commonly used for large-scale carbon nanotube synthesis.[45-46] Nanowires nucleate and grow from seed nanoparticles entrained in a gas flow. The use of a gaseous medium for Aerotaxy permits efficient modulation of reactor composition, thus enabling the fabrication of heterostructures[47] and p-n junctions.[48] However, the unrestricted motion of growing nanowires in a bulk fluid flow renders them susceptible to nanowire-nanowire collisions that can result in irreversible nanowire aggregation. To avoid such deleterious situations, the concentration of nanowires must remain relatively low. By contrast, nanowires produced in the Geode process are prevented from aggregating during growth by their anchoring to the inside wall of the hollow microcapsules.

The design of these hollow microcapsules requires an optimization among competing constraints. Microcapsule diameters of 20 – 70 μm not only provide a large surface area for nanowire growth but are also sufficiently large to prevent microcapsule agglomeration during processing.[49] The microcapsule wall must be porous enough for efficient gas phase transport during nanowire growth, but not so porous that the catalyst seed particles can escape the internal cavity. The hollow microcapsule shell must also be comprised of a material that is thermally stable under VLS growth conditions (T = 400 – 600 ºC) and, depending on the details of the reactor type,[50-51] mechanically robust.

In this paper, we demonstrate two critical components of the Geode process: (1) the scalable production of microcapsules amenable to nanowire growth conditions via emulsion templating and (2) a proof-of-concept demonstration of nanowire growth on the microcapsule interior. While emulsion templating has been used, for example, to encapsulate fertilizers[52] or to create particles for drug delivery,[53-54] the microcapsule requirements outlined above for the Geode

process are quite distinct and necessitate a number of modifications to previously published procedures.[55-57] The fidelity with which intact hollow microspheres can be produced is found to depend on the type of silica particles used as building blocks, and on reinforcement of the microcapsule walls by a polymeric particle cross-linker. We also show that nanowires with morphologies consistent with those possible on flat substrates can be grown on the interior microcapsule surface. The present work sets the stage for future research to achieve and optimize a complete Geode process, including the generation of microcapsules and growth of compositionally-encoded nanowires within, the scalable production free-flowing powders of nanowire-filled microcapsules, as well as harvesting the nanowires therefrom.

Methods

Surface modification of spherical silica particles. Spherical silica particles (Fiber Optic Center Inc, Angström Sphere) with diameters of 250 nm are surface hydrophobized via a procedure adapted from Sander and Studart.[55] The spherical silica particles are dispersed in 20 mL of 2-propanol (IPA, VWR, ≥ 99.5%) to make a 17 wt.% silica suspension. Next, octadecyl(trimethoxy)silane (ODTMS, Sigma-Aldrich, 90%) and 3-aminopropyltriethoxysilane (APTES, Alfa Aesar, 98%) are added to the silica suspension at a mass ratio silica:ODTMS:APTES of 40:5.2:1. The suspension is then sonicated (Biologics Inc., Model 150 V/T) at 20% power and 20% pulse for 2.5 minutes, left to rest for 1 minute, and sonicated again for 2.5 minutes. The resulting suspension is stirred for 24 hours at room temperature. After centrifugation at 4000 rpm for 30 minutes, the supernatant is removed and the surface-modified

silica particles are resuspended in water-saturated dichloromethane (DCM, MilliporeSigma, ≥ 99%). This procedure is repeated 4 times to remove unreacted reagents.

Hollow microcapsule formation via emulsion templating. Hollow microcapsules are produced through a water-in-oil-in-water (W/O/W) double emulsion templating method illustrated in Figure 2 and adapted from Lee and Weitz.[56-57] The first aqueous phase (W_1) contains 1.44 mL of Au nanoparticle dispersion (Ted Pella, 50 nm), 60 μL of 0.5 M NaCl solution (Sigma-Aldrich), and 2 wt.% polyvinyl alcohol (PVA, Sigma-Aldrich, $M_W \sim 31{,}000$). The oil phase (O) consists of 12 wt.% spherical silica particles suspended in water-saturated DCM. A water-in-oil (W_1/O) emulsion is made by combining 3 mL of O and 1.5 mL of W_1, followed by homogenization at 30000 rpm (IKA, T10 Ultra Turrax). For some experiments, 50 μL of 60 wt.% polymeric methylene diphenyl isocyanate (PMDI, Sigma-Aldrich, $\overline{M}_n \sim 400$) in water-saturated DCM is then added to the W_1/O emulsion. PMDI serves as an oil-soluble silica particle cross-linker, reacting with surface hydroxyl groups to create urethane bonds. The second aqueous phase (W_2) consists of 2 wt.% PVA in a 1 mM NaCl solution. For the second emulsification, 8 mL of W_2 are added to the W_1/O single emulsion and the mixture is then vortexed (Scientific Industries, Vortex-Genie 2) for 1 minute. The resulting W_1/O/W_2 double emulsion is left overnight to allow the inner aqueous cores to osmotically swell and coalesce due to the difference in salt concentration between W_1 and W_2. The W_1/O/W_2 emulsion is diluted 20-fold in deionized water to extract the DCM. The hollow microcapsule suspension is air-dried and placed in a calcination oven at 600 °C for 2 hours in air. In some experiments, hydrophobic fumed silica particles (Evonik, Aerosil R812S) are used, instead of spherical silica particles, without further surface modification to produce hollow microcapsules. In this case, the O phase consists of 4 wt.% fumed silica particles in water-saturated DCM and the second vortexing step is performed for 1 minute. All other steps remain the same.

Nanowire growth. Si nanowires are grown inside hollow microcapsules deposited on a Si(100) wafer (University Wafer, 1-10 Ω-cm, single-side polished, boron) in a cold wall chemical vapor deposition reactor (FirstNano, Easy Tube 3000) described previously.[58] Nanowire growth occurs in a two-step procedure. Initial nanowire nucleation occurs at 500 °C for 2 minutes. Nanowire elongation occurs at 480 °C for 10 minutes in the presence of 1000 sccm Hydrogen gas (H_2, AirGas, 99.99%) and 100 sccm Silane (SiH_4, Voltaix, 99.99%) at 10 Torr total reactor pressure.

Characterization. Each step in the emulsion templating process is characterized with optical light microscopy (Nikon Eclipse TE 2000-E) with a 10x objective. A field emission scanning electron microscope (SEM, Zeiss, Ultra60, 5 kV) is used to characterize the morphology of dried microcapsules and as-grown Si nanowires. Focused ion beam milling (FIB, FEI, Nova Nanolab 200, Ga ions, 30 kV) is used to cut through the microcapsule wall and expose the interior. Hollow microcapsules are milled with a current of 20 nA, while microcapsule geodes (i.e., those containing Si nanowires) are milled with a current of 5 nA to minimize nanowire damage.

Results

The steps for producing hollow microcapsules via emulsion templating are outlined in Figure 2. An initial emulsification results in a water-in-oil (W/O) emulsion with hydrophilic metal nanoparticles (that will ultimately seed and catalyze nanowire growth) dispersed in the aqueous droplet phase, and with hydrophobic silica particles (that will ultimately form the microcapsule shell) in the continuous oil phase (Figure 2a). A second emulsification yields a water-in-oil-in-water (W/O/W) double emulsion (Figure 2b). The oil, which is partially soluble in water, is then

extracted into the water phase upon further dilution (Figure 2c). During this extraction step, the silica particles in the oil consolidate to form the porous microcapsule wall. The suspension is dried to yield hollow microcapsules decorated with metal nanoparticles on their interior surfaces (Figure 2d). After calcination, the microcapsules are ready for nanowire growth. Selection of wall nanoparticle type and size enables tuning of the chemical, mechanical, and transport properties of the microcapsules to meet specific process requirements. The energy input during the two emulsification steps provides control over the average microcapsule diameter and wall thickness.

The results from each stage of our emulsion templating process are shown in Figure 2. The first emulsification yields a dense W_1/O single emulsion with W_1 droplets exhibiting diameters of 17 ± 4 μm (Figure 2e). The second emulsification results in a $W_1/O/W_2$ double emulsion where many $W_1/O/W_2$ droplets ultimately contain a single W_1 core (Figure 2f). This morphology results from osmotic swelling and coalescence of multiple internal W_1 cores,[59] driven by the salt concentration gradient between the W_1 and W_2 phases. At this stage, the outer diameter of the $W_1/O/W_2$ droplets is 39 ± 10 μm. Further dilution of the $W_1/O/W_2$ double emulsion with water drives the diffusion of DCM into the outer W_2 phase. As this process proceeds, the silica particles occupying the middle oil phase fully consolidate to form the wall of the hollow microcapsules (Figure 2g) and the outer diameter of the oil-extracted microcapsules reduces to 29 ± 7 μm. The low microcapsule dispersion density observed at this stage results from the large dilution needed to extract the oil. Air drying of the microcapsule suspension on a Si wafer results in a bulk powder (Supporting Information, Figure S1) of spheroidal microcapsules (Figure 2h). We observe holes in the wall of some microcapsules, an effect we attribute to the strong capillary forces that occur during air drying when the air-water interface recedes through the sample. However, such structures also confirm that the microcapsules are indeed hollow. More convincing evidence of the

hollow internal structure of the microcapsules is provided by FIB milling, as shown in Figure 3 for a representative microcapsule. The internal cavity is unobstructed and the wall thickness is 2.2 ± 1.0 μm.

The use of a particle cross-linking agent and choice of silica particle type, as seen in Figure 4, play a major role in maintaining microcapsule integrity during air drying. The use of PMDI as particle cross-linking agent stabilizes the microcapsule wall. Microcapsules dried in the presence of PMDI remain intact upon air drying (Figure 4a) but those dried without PMDI almost entirely collapse (Figure 4b; Supporting Information, Video S1). The use of fumed silica particles (Figure 4c) yields microcapsules with diameters of 24 ± 9 μm and a smoother outer wall than observed for spherical silica particles (Figure 2h). However, even with the use of PMDI, many of fumed silica microcapsules cave-in on themselves during air drying. We hypothesize that this behavior stems from thinner microcapsule walls and/or a lower contact area, and thus weaker adhesion between fumed silica particles. Fumed silica microcapsules, like their spherical silica particle counterparts, fully collapse without the use of PMDI (Figure 4d; Supporting Information, Video S2) during air drying. A detailed examination of these and other emulsification parameters is currently underway in our laboratories.

Si nanowire growth is then completed inside a conventional chemical vapor deposition reactor using conditions common for macroscopic flat substrates. Prior to Si nanowire growth, microcapsules undergo calcination to remove PMDI, the particle cross-linker, and other residual organics which are unfavorable for the reactor and growth conditions. No morphological difference is observed before and after calcination (Supporting Information, Figure S2). Figures 5 and 6 show images of representative geodes following nanowire growth and FIB milling that confirm internal growth of high quality Si nanowires. In order to minimize damage of the interior

nanowires a low FIB current is necessary. A high current mills the microcapsule at a faster rate, but also increases nanowire damage and redeposition of material (Supporting Information, Figure S3). In spite of these artifacts near the FIB cut, a dense network of nanowires with uniform diameters and morphologies is found further away from the opening, inside the capsule (Figure 6). The inset of Figure 6a shows Au nanoparticles at the nanowire tips, which is characteristic of VLS growth. The pinning of the Au nanoparticle near the center of the nanowire tip as well as the untapered nanowire sidewall indicate stable growth and single crystallinity, identical to that possible for growth on flat substrates.[60-63] As-grown nanowires exhibit diameters of 59 ± 10 nm, consistent with the 50 nm seed Au nanoparticles loaded in the W_1 inner aqueous phase. We also observe a small amount of nanowire growth on the microcapsule exterior (Figure 5), an effect we attribute to some Au nanoparticle loss from the inner aqueous core during the second emulsification step.

Discussion

The present work constitutes important first steps toward a complete Geode process, whereby semiconductor nanowires can be grown through the VLS mechanism on the interior surface of hollow, porous microcapsules. Although we initially demonstrate Si nanowire growth inside silica microcapsules, we emphasize that the process is quite general and amenable to a range of materials for both the nanowires (e.g., III-V, II-VI, oxides, etc.) and for microcapsule construction (e.g., Si_3N_4, Al_2O_3, TiO_2). We expect that the efficiency of gas transport through the microcapsule wall will enable the encoding of axial composition profiles similar to that achievable on flat substrates,[64-65] a clear demonstration of which is currently underway in our laboratories.

Future work will aim to understand the differences between nanowire growth on flat substrates and inside hollow microcapsules. For example, the presence of the microcapsule wall likely introduces some heat and mass transport limitations that need to be characterized. Moreover, our bulk emulsion templating process yields a distribution of wall thicknesses (1-3 μm), wall pore sizes (10-100 nm), and/or microcapsule diameters (10-50 μm), which will lead to transport variations from microcapsule to microcapsule. We note that microfluidic devices provide precise control over the emulsion droplet size,[56] but we favor the scale-up offered by bulk emulsion templating methods and expect that the impact of microcapsule structural polydispersity on nanowire growth can be minimized. For example, when operating in a regime where crystal nucleation is rate limiting,[66] the impact of precursor delivery rate can likely be minimized.

A deeper understanding of the relationship between the emulsification process and the properties of the resulting microcapsules is also desired. Air drying is currently being replaced by spray drying in an effort to reduce capillary force-induced damage and collapse of the microcapsule wall currently seen in the fumed silica microcapsules. Microcapsule mechanics must also be understood in order to balance the need for efficient heat and mass transport (i.e., favoring thin and high porosity walls) against the need for microcapsules integrity during processing (i.e., favoring thick and low porosity walls), especially in the packed and fluidized bed reactors that would facilitate process scalability.[50] Relatedly, it will also be important to consider the trade-off between microcapsule integrity and ease of nanowire harvesting after growth, which will likely include mechanical or chemical removal of the microcapsule wall and colloidal stabilization of as-released nanowires.

Conclusion

We demonstrate key steps in the Geode process for the VLS-synthesis of semiconductor nanowires, leveraging the interior of hollow, porous-walled silica microcapsules as a high-surface area substrate. The process starts with the production of hollow silica microcapsules through a water-in-oil-in-water double emulsion templating method. Two different silica particles types as well as the importance of a silica particle cross-linker are studied. Hollow microcapsules produced with spherical silica particles yield microcapsules able to withstand the capillary forces of air drying. As a proof-of-concept, Si nanowires are grown on the microcapsule interior. We believe that the present report of semiconductor nanowire growth using a hollow microcapsule substrate constitutes an important milestone in the development of a new nanomanufacturing process that is ultimately able to produce high quality, and likely structurally complex, nanowires in unprecedented quantities.

FIGURES

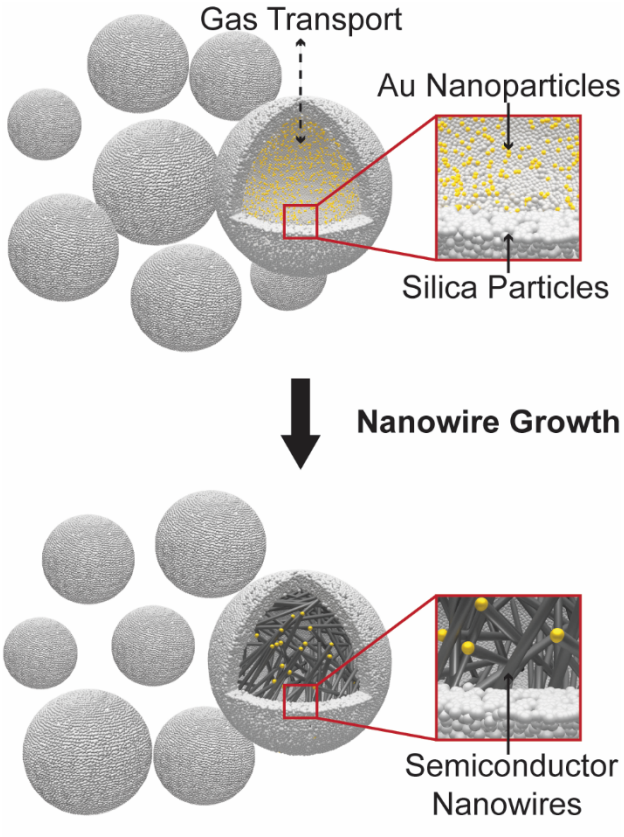

Figure 1. Schematic illustration of the Geode process for the production of semiconductor nanowire synthesis. Hollow, porous-walled microcapsules, which serve as a high surface area substrate for nanowire growth, are produced with a bulk emulsion templating method. The microcapsule interior is lined with the metal nanoparticles that seed nanowire growth via the VLS mechanism. Efficient precursor delivery is enabled by maintaining a porous microcapsule wall. Microcapsule powders can be loaded into a variety of reactor types. The present work demonstrates the Geode process with microcapsules comprised of silica particles and growth of Si nanowires; however, it is compatible with a variety of wall and nanowire materials.

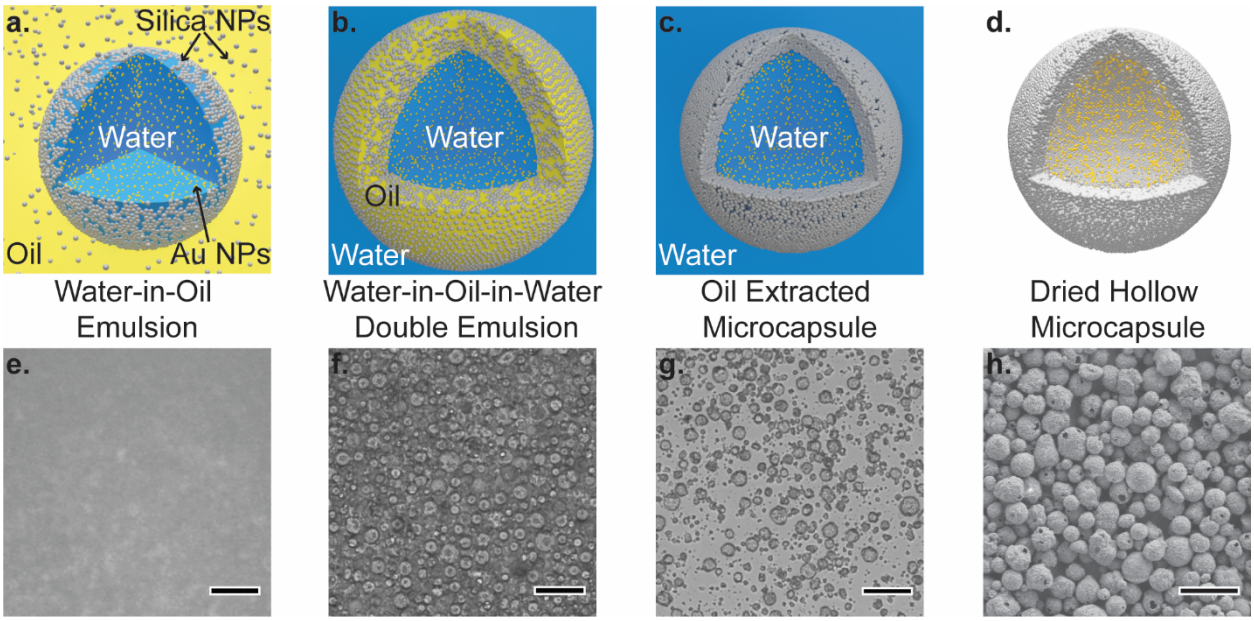

Figure 2. Water-in-oil-in-water ($W_1/O/W_2$) double emulsion templating procedure. Schematics of a (a) water-in-oil (W_1/O) emulsion droplet with Au nanoparticles in the aqueous core and silica particles in the continuous oil phase, (b) $W_1/O/W_2$ double emulsion droplet showing the initial consolidation of the silica particles in the oil phase and Au nanoparticles remaining in the inner aqueous core, (c) oil-extracted microcapsule with a fully consolidated silica particle wall, and (d) dried hollow, porous-walled microcapsule in which Au nanoparticles decorate the interior wall. Representative light microscope images of a (e) W_1/O emulsion, (f) $W_1/O/W_2$ double emulsion, and (g) oil-extracted microcapsule dispersion using spherical silica particles. Scale bars, 100 μm. (h) SEM image of dried hollow microcapsules. Scale bar, 50 μm.

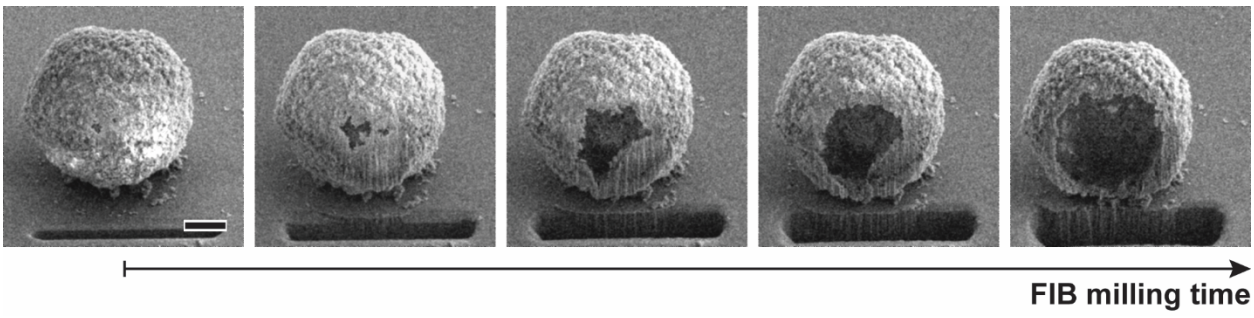

Figure 3. Characterization of hollow microcapsule structure. Image sequence of a representative hollow microcapsule comprised of spherical silica during FIB milling. Overall mill time is 3 minutes. Scale bar, 5 μm.

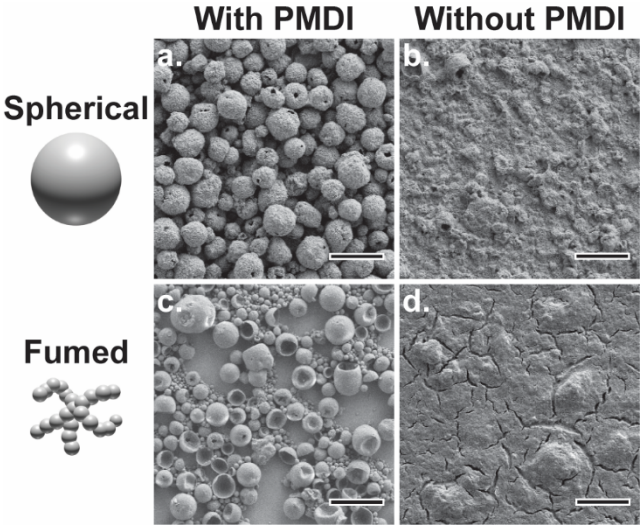

Figure 4. Impact of silica particle type and particle cross-linking agent on microcapsule drying. SEM images of microcapsules comprised of spherical silica particles after air drying (a) with and (b) without PMDI. SEM images of microcapsules comprised of fumed silica particles after air drying (c) with and (d) without PMDI. Scale bar, 50 μm.

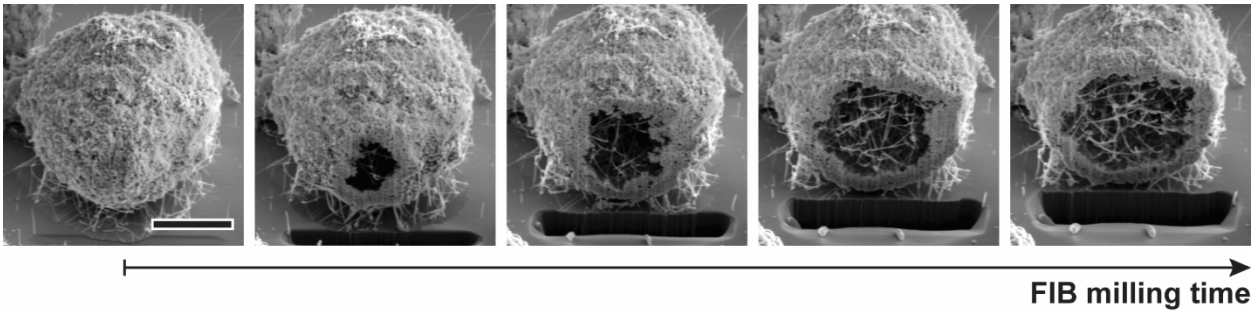

Figure 5. Characterization of nanowire geodes. Image sequence of hollow microcapsules after Si nanowire growth during FIB milling at 5 nA. Overall mill time is 11 minutes. Scale bar, 10 μm. While nanowires near the cut have been damaged by the FIB, good quality nanowires are visible further away (see Figure 6).

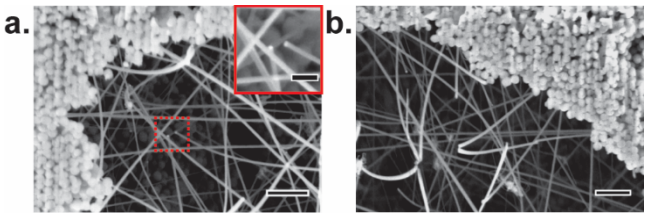

Figure 6. Dense, high quality nanowire growth. (a,b) SEM images of dense Si nanowires inside geodes opened with FIB milling. Scale bars, 1 μm. Inset: Si nanowire tips with visible Au nanoparticles. Scale bar, 300 nm. Nanowires exhibit morphologies analogous to that possible on macroscopic flat substrates.

ASSOCIATED CONTENT

Supporting Information

Additional figures as referenced in the main text. This material is available free of charge via the Internet at http://pubs.acs.org.

AUTHOR INFORMATION

Corresponding Authors

*To whom correspondence should be addressed: mfiller@gatech.edu sbehrens@gatech.edu

Author Contributions

MAF, SHB, and VB conceived of the Geode process. MM conducted emulsion templating experiments and microcapsule characterization. GT and ATM completed nanowire growth. MM, VB, SHB, and MAF designed the experiments, jointly analyzed the data, and wrote the manuscript. All authors approved the final version.

Notes

The authors declare no competing financial interest.

Funding Sources

National Science Foundation

ACKNOWLEDGMENT

The authors gratefully acknowledge the support of the National Science Foundation under Grant No. CBET-1805015. This material is based upon work supported by the National Science Foundation Graduate Research Fellowship under Grant No. DGE-1650044. Any opinions,

findings, and conclusions or recommendations expressed in this material are those of the author(s) and do not necessarily reflect the views of the National Science Foundation. Part of the work at the Georgia Institute of Technology was performed at the Institute for Electronics and Nanotechnology (IEN), a member of the National Nanotechnology Coordinated Infrastructure supported by the National Science Foundation through grant ECCS-1542174.

ABBREVIATIONS

VLS, vapor-liquid-solid; SLS, solution-liquid-solid; W/O, water-in-oil; W/O/W, water-in-oil-in-water; IPA, 2-propanol; ODTMS, octadecyl(trimethoxy)silane; APTES, 3-aminopropyltriethoxysilane; DCM, dichloromethane; W_1, first aqueous phase; Au, Gold; PVA, polyvinyl alcohol; O, oil phase; PMDI, polymeric methylene diphenyl isocyanate; W_2, second aqueous phase; Si, Silicon; SEM, scanning electron microscope; FIB, focus ion beam; H_2, hydrogen gas; SiH_4, silane

REFERENCES

1. Qing, Q.; Jiang, Z.; Xu, L.; Gao, R.; Mai, L.; Lieber, C. M., Free-standing kinked nanowire transistor probes for targeted intracellular recording in three dimensions. *Nature Nanotechnology* **2013,** *9*, 142.

2. Christesen, J. D.; Pinion, C. W.; Hill, D. J.; Kim, S.; Cahoon, J. F., Chemically Engraving Semiconductor Nanowires: Using Three-Dimensional Nanoscale Morphology to Encode Functionality from the Bottom Up. *The Journal of Physical Chemistry Letters* **2016,** *7* (4), 685-692.

3. Kim, S.; Hill, D. J.; Pinion, C. W.; Christesen, J. D.; McBride, J. R.; Cahoon, J. F., Designing Morphology in Epitaxial Silicon Nanowires: The Role of Gold, Surface Chemistry, and Phosphorus Doping. *ACS Nano* **2017,** *11* (5), 4453-4462.

4. Hui, H. Y.; de la Mata, M.; Arbiol, J.; Filler, M. A., Low-Temperature Growth of Axial Si/Ge Nanowire Heterostructures Enabled by Trisilane. *Chemistry of Materials* **2017,** *29* (8), 3397-3402.

5. Wallentin, J.; Anttu, N.; Asoli, D.; Huffman, M.; Åberg, I.; Magnusson, M. H.; Siefer, G.; Fuss-Kailuweit, P.; Dimroth, F.; Witzigmann, B.; Xu, H. Q.; Samuelson, L.; Deppert, K.; Borgström, M. T., InP Nanowire Array Solar Cells Achieving 13.8% Efficiency by Exceeding the Ray Optics Limit. *Science* **2013,** *339* (6123), 1057-1060.

6. Fuhrer, A.; Fröberg, L. E.; Pedersen, J. N.; Larsson, M. W.; Wacker, A.; Pistol, M.-E.; Samuelson, L., Few Electron Double Quantum Dots in InAs/InP Nanowire Heterostructures. *Nano Letters* **2007,** *7* (2), 243-246.

7. Cui, Y.; Lieber, C. M., Functional Nanoscale Electronic Devices Assembled Using Silicon Nanowire Building Blocks. *Science* **2001,** *291* (5505), 851.

8. Colinge, J.-P.; Lee, C.-W.; Afzalian, A.; Akhavan, N. D.; Yan, R.; Ferain, I.; Razavi, P.; O'Neill, B.; Blake, A.; White, M.; Kelleher, A.-M.; McCarthy, B.; Murphy, R., Nanowire transistors without junctions. *Nature Nanotechnology* **2010,** *5*, 225.

9. Wu, Y.; Xiang, J.; Yang, C.; Lu, W.; Lieber, C. M., Single-crystal metallic nanowires and metal/semiconductor nanowire heterostructures. *Nature* **2004,** *430* (6995), 61-65.

10. Björk, M. T.; Schmid, H.; Knoch, J.; Riel, H.; Riess, W., Donor deactivation in silicon nanostructures. *Nature Nanotechnology* **2009,** *4*, 103.

11. Yang, C.; Barrelet, C. J.; Capasso, F.; Lieber, C. M., Single p-Type/Intrinsic/n-Type Silicon Nanowires as Nanoscale Avalanche Photodetectors. *Nano Letters* **2006,** *6* (12), 2929-2934.

12. Fan, P.; Chettiar, U. K.; Cao, L.; Afshinmanesh, F.; Engheta, N.; Brongersma, M. L., An invisible metal–semiconductor photodetector. *Nature Photonics* **2012,** *6*, 380.

13. Cao, L.; White, J. S.; Park, J.-S.; Schuller, J. A.; Clemens, B. M.; Brongersma, M. L., Engineering light absorption in semiconductor nanowire devices. *Nature Materials* **2009,** *8*, 643.

14. Peng, K.; Xu, Y.; Wu, Y.; Yan, Y.; Lee, S.-T.; Zhu, J., Aligned Single-Crystalline Si Nanowire Arrays for Photovoltaic Applications. *Small* **2005,** *1* (11), 1062-1067.

15. Tsakalakos, L.; Balch, J.; Fronheiser, J.; Korevaar, B. A.; Sulima, O.; Rand, J., Silicon nanowire solar cells. *Applied Physics Letters* **2007,** *91* (23), 233117.

16. Garnett, E.; Yang, P., Light Trapping in Silicon Nanowire Solar Cells. *Nano Letters* **2010,** *10* (3), 1082-1087.

17. Krogstrup, P.; Jørgensen, H. I.; Heiss, M.; Demichel, O.; Holm, J. V.; Aagesen, M.; Nygard, J.; Fontcuberta I Morral, A., Single-nanowire solar cells beyond the Shockley-Queisser limit. *Nature Photonics* **2013,** *7* (4), 306-310.

18. Hochbaum, A. I.; Chen, R.; Delgado, R. D.; Liang, W.; Garnett, E. C.; Najarian, M.; Majumdar, A.; Yang, P., Enhanced thermoelectric performance of rough silicon nanowires. *Nature* **2008,** *451* (7175), 163-167.

19. Borgström, M. T.; Wallentin, J.; Heurlin, M.; Fält, S.; Wickert, P.; Leene, J.; Magnusson, M. H.; Deppert, K.; Samuelson, L., Nanowires With Promise for Photovoltaics. *IEEE Journal of Selected Topics in Quantum Electronics* **2011,** *17* (4), 1050-1061.

20. Kim, S.-K.; Zhang, X.; Hill, D. J.; Song, K.-D.; Park, J.-S.; Park, H.-G.; Cahoon, J. F., Doubling Absorption in Nanowire Solar Cells with Dielectric Shell Optical Antennas. *Nano Letters* **2015,** *15* (1), 753-758.

21. Schmidt, V.; Wittemann, J. V.; Senz, S.; Gösele, U., Silicon Nanowires: A Review on Aspects of their Growth and their Electrical Properties. *Advanced Materials* **2009,** *21* (25-26), 2681-2702.

22. Fan, Z.; Ho, J. C.; Jacobson, Z. A.; Yerushalmi, R.; Alley, R. L.; Razavi, H.; Javey, A., Wafer-Scale Assembly of Highly Ordered Semiconductor Nanowire Arrays by Contact Printing. *Nano Letters* **2008,** *8* (1), 20-25.

23. Wakayama, Y.; Tanaka, S.-i., Kinetics of surface droplet epitaxy and its application to fabrication of mushroom-shaped metal/Si heterostructure on nanometer scale. *Surface Science* **1999,** *420* (2), 190-199.

24. Weyher, J., The liquid surface tension as a factor influencing the VLS growth of silicon crystals. *Materials Science and Engineering* **1975,** *20*, 171-177.

25. Hu, Q.; Wu, H.; Sun, J.; Yan, D.; Gao, Y.; Yang, J., Large-area perovskite nanowire arrays fabricated by large-scale roll-to-roll micro-gravure printing and doctor blading. *Nanoscale* **2016,** *8* (9), 5350-5357.

26. Pan, C.; Luo, Z.; Xu, C.; Luo, J.; Liang, R.; Zhu, G.; Wu, W.; Guo, W.; Yan, X.; Xu, J.; Wang, Z. L.; Zhu, J., Wafer-Scale High-Throughput Ordered Arrays of Si and Coaxial Si/Si1–xGex Wires: Fabrication, Characterization, and Photovoltaic Application. *ACS Nano* **2011,** *5* (8), 6629-6636.

27. Yeon, J.; Lee, Y. J.; Yoo, D. E.; Yoo, K. J.; Kim, J. S.; Lee, J.; Lee, J. O.; Choi, S.-J.; Yoon, G.-W.; Lee, D. W.; Lee, G. S.; Hwang, H. C.; Yoon, J.-B., High Throughput Ultralong (20 cm) Nanowire Fabrication Using a Wafer-Scale Nanograting Template. *Nano Letters* **2013,** *13* (9), 3978-3984.

28. geode. In *Dictionary of Gems and Gemology*, Manutchehr-Danai, M., Ed. Springer Berlin Heidelberg: Berlin, Heidelberg, 2009; pp 380-380.

29. Rakovan, J., Word to the Wise: Geode (and Friends). *Rocks & Minerals* **2017,** *92* (1), 85-91.

30. Rossier-Miranda, F. J.; Schroën, C. G. P. H.; Boom, R. M., Colloidosomes: Versatile microcapsules in perspective. *Colloids and Surfaces A: Physicochemical and Engineering Aspects* **2009,** *343* (1), 43-49.

31. Corma, A.; Garcia, H., Supported gold nanoparticles as catalysts for organic reactions. *Chemical Society Reviews* **2008,** *37* (9), 2096-2126.

32. Costa, N. J. S.; Rossi, L. M., Synthesis of supported metal nanoparticle catalysts using ligand assisted methods. *Nanoscale* **2012,** *4* (19), 5826-5834.

33. Vogt, E. T. C.; Weckhuysen, B. M., Fluid catalytic cracking: recent developments on the grand old lady of zeolite catalysis. *Chemical Society Reviews* **2015,** *44* (20), 7342-7370.

34. Wank, J. R.; George, S. M.; Weimer, A. W., Vibro-fluidization of fine boron nitride powder at low pressure. *Powder Technology* **2001,** *121* (2), 195-204.

35. Hanrath, T.; Korgel, B. A., Supercritical Fluid–Liquid–Solid (SFLS) Synthesis of Si and Ge Nanowires Seeded by Colloidal Metal Nanocrystals. *Advanced Materials* **2003,** *15* (5), 437-440.

36. Lu, X.; Hanrath, T.; Johnston, K. P.; Korgel, B. A., Growth of Single Crystal Silicon Nanowires in Supercritical Solution from Tethered Gold Particles on a Silicon Substrate. *Nano Letters* **2003,** *3* (1), 93-99.

37. Grebinski, J. W.; Hull, K. L.; Zhang, J.; Kosel, T. H.; Kuno, M., Solution-Based Straight and Branched CdSe Nanowires. *Chemistry of Materials* **2004,** *16* (25), 5260-5272.

38. Sun, J.; Liu, C.; Yang, P., Surfactant-Free, Large-Scale, Solution–Liquid–Solid Growth of Gallium Phosphide Nanowires and Their Use for Visible-Light-Driven Hydrogen Production from Water Reduction. *Journal of the American Chemical Society* **2011,** *133* (48), 19306-19309.

39. Wang, F.; Dong, A.; Sun, J.; Tang, R.; Yu, H.; Buhro, W. E., Solution−Liquid−Solid Growth of Semiconductor Nanowires. *Inorganic Chemistry* **2006,** *45* (19), 7511-7521.

40. Lu, X.; Fanfair, D. D.; Johnston, K. P.; Korgel, B. A., High Yield Solution−Liquid−Solid Synthesis of Germanium Nanowires. *Journal of the American Chemical Society* **2005,** *127* (45), 15718-15719.

41. Heurlin, M.; Magnusson, M. H.; Lindgren, D.; Ek, M.; Wallenberg, L. R.; Deppert, K.; Samuelson, L., Continuous gas-phase synthesis of nanowires with tunable properties. *Nature* **2012,** *492* (7427), 90-94.

42. Zhang, W.; Yang, F. F.; Messing, M. E.; Mergenthaler, K.; Pistol, M. E.; Deppert, K.; Samuelson, L.; Magnusson, M. H.; Yartsev, A., Recombination dynamics in aerotaxy-grown Zn-doped GaAs nanowires. *Nanotechnology* **2016,** *27* (45).

43. Metaferia, W.; Persson, A. R.; Mergenthaler, K.; Yang, F. F.; Zhang, W.; Yartsev, A.; Wallenberg, R.; Pistol, M. E.; Deppert, K.; Samuelson, L.; Magnusson, M. H., GaAsP Nanowires Grown by Aerotaxy. *Nano Letters* **2016,** *16* (9), 5701-5707.

44. Najmi, Z.; Ebrahimipour, G.; Franzetti, A.; Banat, I. M., In situ downstream strategies for cost-effective bio/surfactant recovery. *Biotechnology and Applied Biochemistry* **2018,** *65* (4), 523-532.

45. Cheng, H. M.; Li, F.; Su, G.; Pan, H. Y.; He, L. L.; Sun, X.; Dresselhaus, M. S., Large-scale and low-cost synthesis of single-walled carbon nanotubes by the catalytic pyrolysis of hydrocarbons. *Applied Physics Letters* **1998,** *72* (25), 3282-3284.

46. Cheng, H. M.; Li, F.; Sun, X.; Brown, S. D. M.; Pimenta, M. A.; Marucci, A.; Dresselhaus, G.; Dresselhaus, M. S., Bulk morphology and diameter distribution of single-walled carbon nanotubes synthesized by catalytic decomposition of hydrocarbons. *Chemical Physics Letters* **1998,** *289* (5), 602-610.

47. Zhang, W.; Yang, F.; Messing, M. E.; Mergenthaler, K.; Pistol, M.-E.; Deppert, K.; Samuelson, L.; Magnusson, M. H.; Yartsev, A., Recombination dynamics in aerotaxy-grown Zn-doped GaAs nanowires. *Nanotechnology* **2016,** *27* (45), 455704.

48. Barrigón, E.; Hultin, O.; Lindgren, D.; Yadegari, F.; Magnusson, M. H.; Samuelson, L.; Johansson, L. I. M.; Björk, M. T., GaAs Nanowire pn-Junctions Produced by Low-Cost and High-Throughput Aerotaxy. *Nano Letters* **2018,** *18* (2), 1088-1092.

49. Kunii, D.; Levenspiel, O., *Fluidization engineering*. 2nd ed. ed.; Butterworth-Heinemann: Boston, 1991.

50. King, D. M.; Spencer, J. A.; Liang, X.; Hakim, L. F.; Weimer, A. W., Atomic layer deposition on particles using a fluidized bed reactor with in situ mass spectrometry. *Surface and Coatings Technology* **2007,** *201* (22), 9163-9171.

51. King, D. M.; Liang, X.; Weimer, A. W., Functionalization of fine particles using atomic and molecular layer deposition. *Powder Technology* **2012,** *221*, 13-25.

52. França, D.; Medina, Â. F.; Messa, L. L.; Souza, C. F.; Faez, R., Chitosan spray-dried microcapsule and microsphere as fertilizer host for swellable − controlled release materials. *Carbohydrate Polymers* **2018,** *196*, 47-55.

53. Lim, M. P. A.; Lee, W. L.; Widjaja, E.; Loo, S. C. J., One-step fabrication of core–shell structured alginate–PLGA/PLLA microparticles as a novel drug delivery system for water soluble drugs. *Biomaterials Science* **2013,** *1* (5), 486-493.

54. Finnie, K. S.; Waller, D. J.; Perret, F. L.; Krause-Heuer, A. M.; Lin, H. Q.; Hanna, J. V.; Barbé, C. J., Biodegradability of sol–gel silica microparticles for drug delivery. *Journal of Sol-Gel Science and Technology* **2009,** *49* (1), 12-18.

55. Sander, J. S.; Studart, A. R., Multiwalled functional colloidosomes made small and in large quantities via bulk emulsification. *Soft Matter* **2014,** *10* (1), 60-68.

56. Lee, D.; Weitz, D. A., Double Emulsion-Templated Nanoparticle Colloidosomes with Selective Permeability. *Advanced Materials* **2008,** *20* (18), 3498-3503.

57. Lee, D.; Weitz, D. A., Nonspherical Colloidosomes with Multiple Compartments from Double Emulsions. *Small* **2009,** *5* (17), 1932-1935.

58. Musin, I. R.; Filler, M. A., Chemical Control of Semiconductor Nanowire Kinking and Superstructure. *Nano Letters* **2012,** *12* (7), 3363-3368.

59. Shitta, A. Morphology Control for Particle Stabilized Droplets and Droplet Templated Microcapsules. Doctoral, Georgia Institute of Technology, Georgia Institute of Technology, 2015.

60. Cui, Y.; Lauhon, L. J.; Gudiksen, M. S.; Wang, J.; Lieber, C. M., Diameter-controlled synthesis of single-crystal silicon nanowires. *Applied Physics Letters* **2001,** *78* (15), 2214-2216.

61. Wu, Y.; Cui, Y.; Huynh, L.; Barrelet, C. J.; Bell, D. C.; Lieber, C. M., Controlled Growth and Structures of Molecular-Scale Silicon Nanowires. *Nano Letters* **2004,** *4* (3), 433-436.

62. Hochbaum, A. I.; Fan, R.; He, R.; Yang, P., Controlled Growth of Si Nanowire Arrays for Device Integration. *Nano Letters* **2005,** *5* (3), 457-460.

63. Schmid, H.; Björk, M. T.; Knoch, J.; Riel, H.; Riess, W.; Rice, P.; Topuria, T., Patterned epitaxial vapor-liquid-solid growth of silicon nanowires on Si(111) using silane. *Journal of Applied Physics* **2008,** *103* (2), 024304.

64. Gudiksen, M. S.; Lauhon, L. J.; Wang, J.; Smith, D. C.; Lieber, C. M., Growth of nanowire superlattice structures for nanoscale photonics and electronics. *Nature* **2002,** *415* (6872), 617-620.

65. Yang, C.; Zhong, Z.; Lieber, C. M., Encoding Electronic Properties by Synthesis of Axial Modulation-Doped Silicon Nanowires. *Science* **2005,** *310* (5752), 1304.

66. Pinion, C. W.; Nenon, D. P.; Christesen, J. D.; Cahoon, J. F., Identifying Crystallization- and Incorporation-Limited Regimes during Vapor–Liquid–Solid Growth of Si Nanowires. *ACS Nano* **2014,** *8* (6), 6081-6088.

TOC Graphic

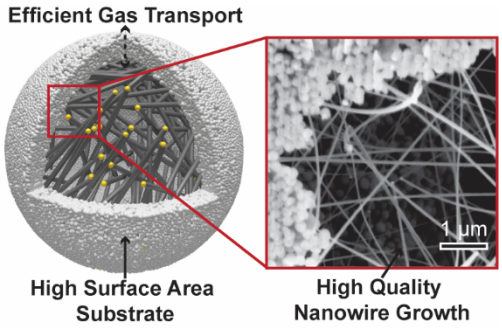
Efficient Gas Transport
1 um
High Surface Area Substrate
High Quality Nanowire Growth

SUPPORTING INFORMATION

The Geode Process I: Hollow Silica Microcapsules as a High Surface Area Substrate for Semiconductor Nanowire Growth

Maritza Mujica, Gozde Tutuncuoglu, Amar T. Mohabir, Victor Breedveld, Sven H. Behrens and Michael A. Filler**

School of Chemical & Biomolecular Engineering, Georgia Institute of Technology, Atlanta 30332, Georgia, United States

* E-mail: michael.filler@chbe.gatech.edu, sven.behrens@chbe.gatech.edu

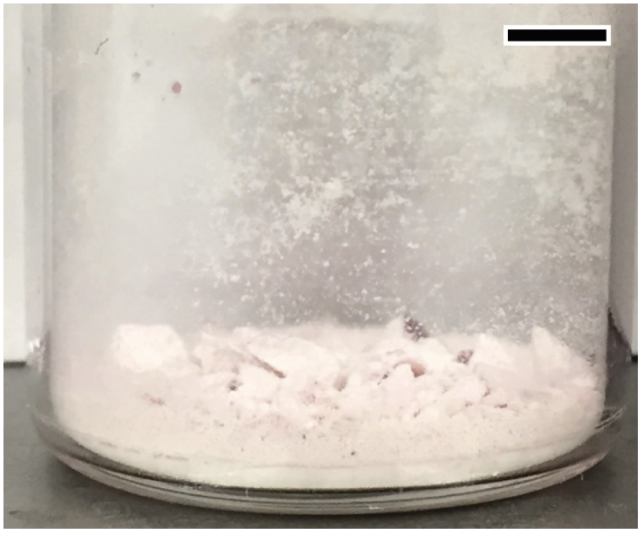

Figure S1. Air dried silica microcapsules containing spherical silica particles. Scale bar, 5 mm.

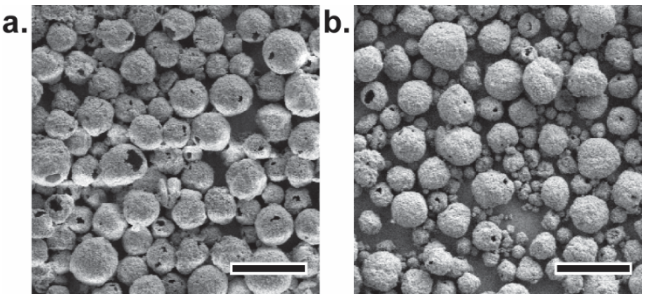

Figure S2. Calcination of hollow silica microcapsules. Silica microcapsules containing spherical silica particles (a) before and (b) after calcination at 600 °C in air for 2 hours. Scale bars, 50 μm.

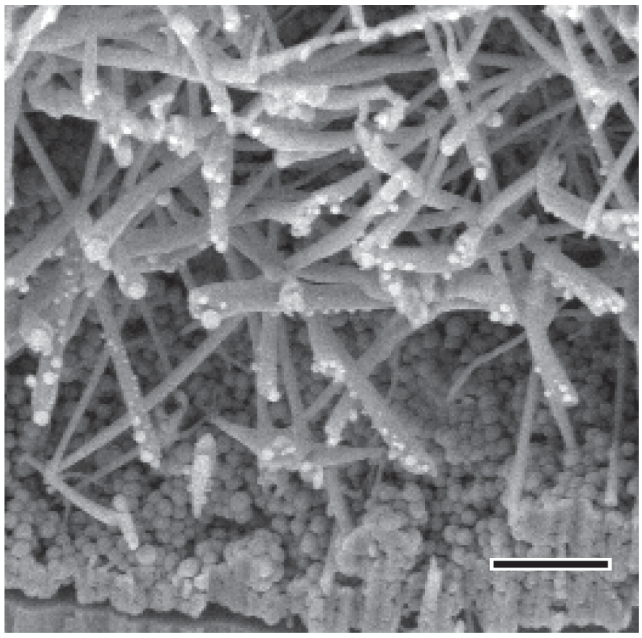

Figure S3. Focused ion beam damage. High currents result in damage to and redeposition on Si nanowires inside microcapsules. Scale bar, 2 μm.

Supplementary Video Captions

Video S1. Light microscope (40x objective, 32x speed) observation of spherical silica microcapsules air drying without PMDI. Scale bar, 20 μm.

Video S2. Light microscope (40x objective, 32x speed) observation of fumed silica microcapsules air drying without PMDI. Scale bar, 10 μm.